Supporting information

Relieving Immunosuppression by Endo@PLT Targeting Anti-angiogenesis to Improve the Efficacy of Immunotherapies

Chao Chen, [a] † Yijie Tang, [C] † Hao Huang, [a] Li Jia, [a] Lingzi Feng, [a] Jianya Zhao, [a] Hao Zhang,[e] Jian He,[d]* Lingchi Ding, [b]* and Donglin Xia [a]*

[a] School of Public Health, Nantong University, Nantong, Jiangsu 226019, China

[b] Affiliated Tumor Hospital of Nantong University, Nantong, Jiangsu 226361, China

[c] Affiliated Hospital of Nantong University, Nantong, Jiangsu 226001, China

[d] Department of Radiology, Nanjing Drum Tower Hospital, the Affiliated Hospital of Nanjing University Medical School, Nanjing, Jiangsu 210008, China.

[e] Department of oncology, the first Affiliated Hospital of Nanjing Medical University, Nanjing, Jiangsu 210029, China.

Corresponding authors: hjxueren@126.com (J. He), dinglingchi@139.com (L.C. Ding), xiadonglin@ntu.edu.cn (D.L. Xia)

1. EXPERIMENTAL SECTION

Materials. Endostar (Endo) was supplied by Xiansheng Pharmaceutical Co., Ltd (Shandong, China). PD-1 was provided by Hengrui Pharmaceutical Co., Ltd (Jiangsu, China). Prostaglandin E1 (PGE1), and fluorescent dyes (such as FITC, Rhodamine B) were purchased from Beyotime Biotechnology Co., LTD. (Shanghai, China). Cyanine5 Carboxylic Acid (Cy5) was purchased from Bioorth Biotech Co., Ltd. (Jiangsu, China). CD31 polyclonal antibody was brought from Abbkine Scientific Co., Ltd. (CA, USA). Tumor necrosis factor-α (TNF-α) was purchased from Bomei Biotechnology (Guangzhou, China) and used according to the manufacturer's instructions. Hoechst 33342 staining solution for live cells, were purchased from Beijing Biosynthesis Biotechnology Co., LTD. (Beijing, China). All other reagents were analytical grade and used without further purification/modification.

Animals and cell culture. Ten SPF Sprague Dawley (SD) rats and C57BL/6 mice (six weeks old) were purchased from the Experimental Animal Center of Nantong University, China. All the animals were housed under specific pathogen-free conditions and used under approved protocols. Blood was collected from SD rats by heart puncture into sodium citrate (3.2%).

Lewis's lung cancer (LLC) cells and Bronchial Epithelium transformed with Ad12-SV40 2B (BEAS-2B) were purchased from Suer Biotech Co., Ltd. (Shanghai, China). All media were supplemented with 10% fetal bovine serum and 100 IU/mL penicillin G sodium, 100 μg/mL streptomycin sulfate. LLC cells were cultured in a humid air atmosphere with 5% (v/v) CO_2 at 37 °C. The Helsinki Declaration of 1975 was followed.

Platelet isolation. Platelets were isolated according to a previously described method.[1] Briefly, blood was drawn into ACD EDTAK2-tubes for platelet isolation and centrifuged (200 g for 20 min, at room temperature) to obtain platelet-rich plasma. Then, 20 μg prostaglandin E1 (PGE1) was included to prevent aggregation of the platelet.

Synthesis of Endo@PLT. To prepare Endo@PLT, Endo was mixed with PLT, and the mixture was sonicated for about 10 min with in FS30D bath sonicator (30 W).

Subsequently, the mixture was collected by centrifugation at 3,000 r/min for 10 min. The obtained Endo@PLT complex was dispersed in 1 mL PBS containing PGE1. The unbound Endo was removed and washed three times by centrifugation at 3000 r/min for 5min. The concentration of Endo was determined by ELISA assay kit (Enzyme-linked Biotechnology, China) according to the manufacturer's instructions. The absorbance of samples was measured at 450 nm within 10 min. Experiments were repeated at least three times.

Characterization. The SEM characterization was performed on the JSM-6700F (Jeol Ltd, Tokyo, Japan) scanning electron microscope. The zeta-potential changes of Endo@PLT were measured using Zetasizer (Nano ZS90, Worcestershire, UK). The Ultraviolet-visible (UV-Vis) absorption spectra of Endo@PLT were recorded on Shimadzu UV-2450 UV–vis spectrometer at 350-700 nm range. The Endo encapsulation efficiency and drug loading efficiency in PLT were calculated as earlier reported.[1] After the Endo was labeled with Rhodamine B dye (red) and PLT was stained by FITC, the Endo@PLT was prepared as previously described. Laser confocal pictures of Endo@PLT were performed on a Leica TCS SP8 STED 3X microscope.

Tumor targeted behavior. To further examine whether Endo@PLT may have efficiently targeted to the tumor and aggregated, ADP (10 μM) was used as an activator of Endo@PLT particles. The SEM imaging morphology characterization was carried out after the ADP (0 or 10 μM) was added into 1 mL Endo@PLT.

The BEAS-2B cells were used as normal control and LLC cells were used as tumor group. After the Endo@PLT (red rhodamine modified Endo) cultured with BEAS-2B or LLC cells for 24 h, the media was removed, and washed with PBS. Then the cells were fixed with 4% paraformaldehyde. Washed cells were stained with Hoechst 33342 to highlight the nuclei, and images were taken on FV 3000 confocal laser scanning microscopy (Olympus, Tokyo, Japan). Dynamic changes in cells' fluorescence intensity were measured using a Shimadzu RF-5301 PC spectrophotometer (Shimadzu, Tokyo, Japan).

Dose selection. The 7.5 mg/m^2/day dose is the Endo used in clinical based on the manufacturer instructions.[2] According to the surface area of the Sprague Dawley rat is about 0.003 m^2 and the time of Endo treatment is 7 days, the total amount of Endo administered is about 0.14 mg. From the results in Figure 1, the concentration of Endo in the Endo@PLT was 0.72 mg/mL, which was used in the animal experiments. Therefore, 200μL Endo@PLT was chosen as the dose of intravenous administration in the animal experiments.

The construction of tumor model. The LLC tumor model was established via the tail vein injection of LLC cells (100 μL, 1×10^6 cells) into the C57BL/6 mice. CT examinations were performed using a 64-slice CT scanner (Somatom Definition Flash, MA, USA) to determine whether the model was successfully prepared.

***In vivo* imaging.** For *in vivo* imaging, we used a PerkinElmer IVIS Lumina Series III *ex/in vivo* imaging system (Waltham, MA, USA). First, to demonstrate the effectiveness of PLT carrier in drug deliver to the tumor, the PLT was labeled with Cy5 and the *in vivo* distribution was examined by in vivo imaging experiments. Then the Endo was labeled with Cy5 and used in Endo@PLT preparation. Ten mice were anesthetized and injected with free Endo or Endo@PLT. After 6 h, all mice were sacrificed, and major organs including heart, liver, spleen, lungs (tumor), and kidneys were collected for *ex vivo* imaging.

***In vivo* experiments.** Fifty tumor-bearing mice were randomly divided into five groups and treated through tail-vein injection. (1) Negative control: treated with 200 μL PBS at day 1. (2) Endo 200 μL free Endo (5 mg/mL) treated at day 1. (3) PLT, 200 μL PLT treated at day 1. (4) Endo + PLT group, 1mg free Endo mixed with PLT and treated at day 1. (4) Endo@PLT group, 200 μL Endo@PLT treated at day 1. After 7 days, mice in each group were sacrificed to investigate hypoxia. The lung sections were stained with hematoxylin and eosin and immune-stained for VEGF and CD31 measurements. The anti-tumor effect and targetability of Endo@PLT particles *in vivo* were studied.

***In vivo* antitumor efficacy.** Fouty tumor-bearing mice were randomly divided into five groups and treated through tail-vein injection. (1) Negative control: treated with 200 μL PBS at day 1; (2) PD-1 group, 10 mg/kg PD-1 treated at day 1; (3) Free Endo + PD-1 group, 200 μL free Endo treated at day 1, and then PD-1(10mg/kg) was administered at day 7. (4) Endo@PLT + PD-1 group, 200 μL Endo@PLT treated at day 1, and then PD-1(10mg/kg) was administered at day 7.

After mice were treated with PBS, PD-1, free Endo + PD-1 or Endo@PLT + PD-1, survival rates and the number of metastatic nodules in each group were recorded. After 60 days, mice in each group were sacrificed to investigate hypoxia, tumor apoptosis, and necrosis. The lung sections were stained with hematoxylin and eosin and immune-stained for VEGF and CD31 measurements.

Immunohistochemistry of the mice lung sections and immunofluorescence staining of $CD8^+$ and IFN-γ in the LLC tumors were performed in the Histomorphology Platform, Nantong University, following standard protocols. For the immunofluorescence staining of CD8a, the Alexa Fluor 647 anti-mouse CD8a (BioLegend, catalog no. 100724, CA, USA) 1:50 antibody was used. For immunofluorescence staining of IFN-γ, an IFN-γ primary antibody (Thermo Fisher Scientific, catalog no. PA5-20390, 1:50) and an Alexa Fluor 647-labeled second antibody (BD Co., A0468, 1:100) were used.

Immunofluorescent staining was performed using the interleukin (IL)-17, anti-TNF-β1 antibodies. The nuclei were counterstained with 4′,6-diamidino-2-phenylindole, and slides were mounted with Prolong Gold Anti-fade reagent (Life Technologies, CA, USA). The Image J software determined the average pixel count for each fluorescent channel and calculated a positive: negative pixel expression ratio in the visualized area of tissue

Long-Term Cytotoxicity. C57BL/6 mice that received an Endo@PLT+PD-1 *i.v.* were sacrificed on days 30 or 60. In this experiment, the mice were sacrificed, histological structures of heart, liver, kidney, and spleen were collected and determined by standard hematoxylin-eosin (HE) staining. Whole blood was collected and the

erythrocytes (RBC), white blood cells (WBC), platelets (PLT), and hemoglobin (HGB) were detected using the animal hematology analyzer. Serum samples were obtained by centrifuging 2 mL of whole blood at 2,500 rpm for 15 min. Alanine aminotransferase (ALT), aspartic aminotransferase (AST), alkaline phosphatase (ALP), creatinine (CR), blood urea nitrogen (BUN), and globulin (GLB) were detected by the Trilogy automatic biochemical analyzer (tri-9002, TX, USA).

Statistical analysis. The SPSS 21.0 statistical software was used for statistical analysis. The one-way ANOVA and Dunnett's multiple comparisons test were used for multiple-group comparisons, while Student's *t*-test evaluated the significance between two groups. A value of $P < 0.05$ was considered statistically significant.

2. RESULTS

The SEM and hydrodynamic size distribution results of Endo and PLT was shown in Fig. S1. The Endo particle size was about 10 nm. The Endo were approximately round, while PLT showed an indefinite shape. The PLT particle size was 989-1121 nm (Fig. S1B).

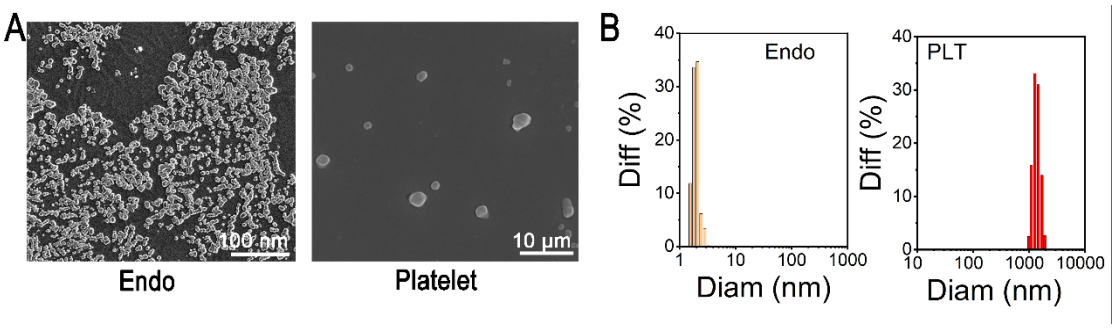

Fig. S1 (A) SEM and (B) hydrodynamic size distribution of the Endo and PLT.

Cytotoxicity assays are essential for the initial phases of antitumor drug development.[3] PLT, Endo, and Endo@PLT exhibited less cytotoxicity, reflecting good compatibility (Fig. S2A). The UV absorbance of hemoglobin also evaluated the hemolysis ratio. The recommended hemolysis ratio for intravenous injection is <5%.[4] The hemolysis ratios of PLT, Endo, and Endo@PLT was <4%, indicating that Endo@PLT is suitable for intravenous injection (Fig. S1B). Moreover, the Endo@PLT achieved stability after seven days (Fig. S2C).

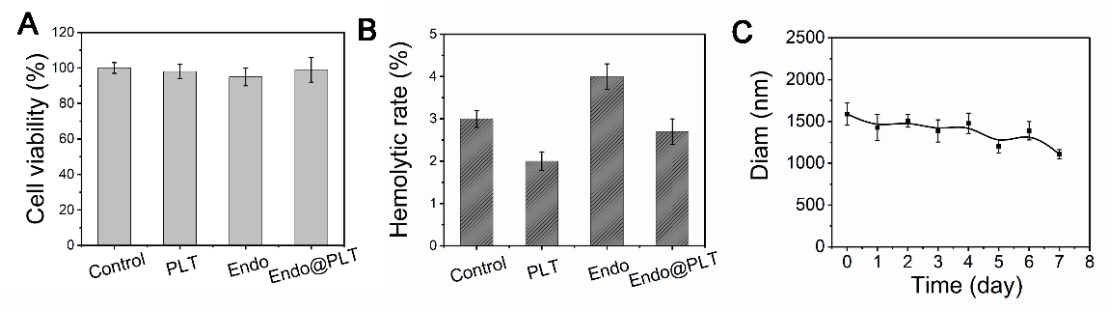

Fig. S2 Characterization of the Endo@PLT. (A) Cytotoxicity test, (B) Hemolytic test, and (C) Biostability.

After drug loading, the unbound Endo was removed and washed three times by centrifugation. As shown in Fig. S3, most of the unbound Endo were removed from the Endo@PLT.

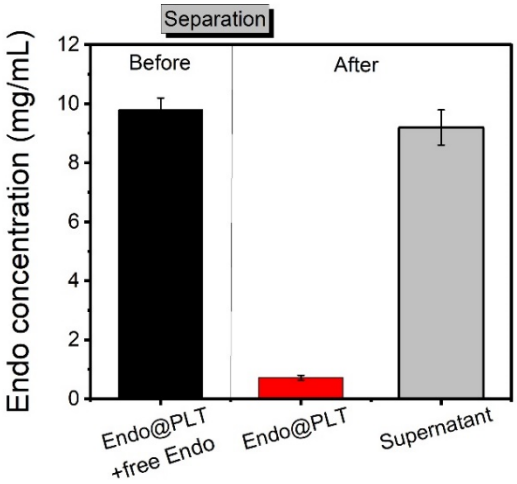

Fig. S3 The Endo concentration in the Endo@PLT before and after septation.

In this study, to further examine whether Endo@PLT may have efficiently targeted to the tumor and aggregated, ADP (10 μM) was used as an activator of Endo@PLT particles (Fig. S4). According to previous studies,[5] the rationale of platelets response to ADP was that the shape change and transient aggregation occurs upon activation of ADP-activated P2Y1 and P2Y12 receptors by the ADP.

To prove that branching happens in Endo@PLT by ADP due to its activation, the Endo@PLT aggregation was restudied and the Endo@PLT without treated with ADT was set as the control. From Fig. S4, it is evident that the Endo@PLT could be activated by the ADT. After the ADP was added for about 5 min, the branching happened in

Endo@PLT and then released contents at about 10 min. However, there were no changes in the Endo@PLT without being activated by ADP.

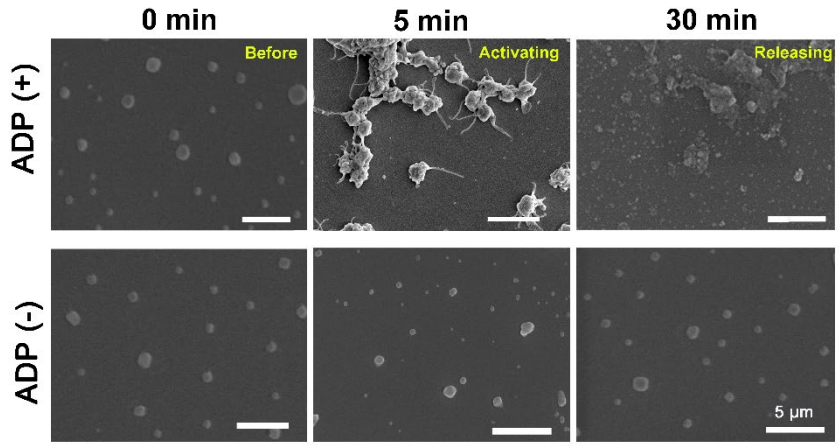

Fig. S4 The global image of activating Endo@PLT. It is evident that the Endo@PLT could be activated by the ADP. After the addition for about 5 min, the branching happened in Endo@PLT and then released contents at about 10 min. However, there were no changes in the Endo@PLT without being activated by ADP.

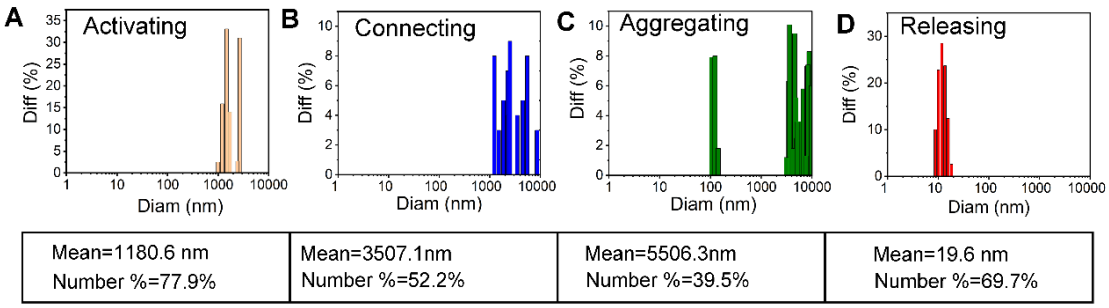

Fig. S5 The hydrodynamic size distrbution of Endo@PLT during the activation process.

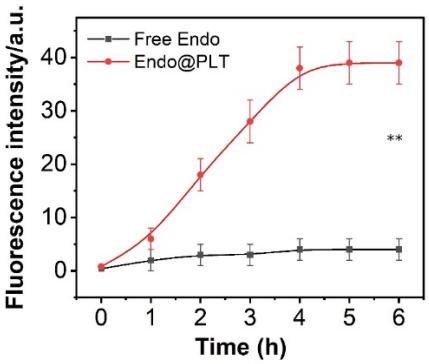

Fig. S6 The fluorescence intensity analysis of BEAS-2B and LLC cells after Endo@PLT treatment. The LLC cells treated with free Endo showed very little red fluorescence. The fluorescence intensity was 8.6-fold higher in the Endo@PLT treatment ($P<0.01$) than the free Endo.

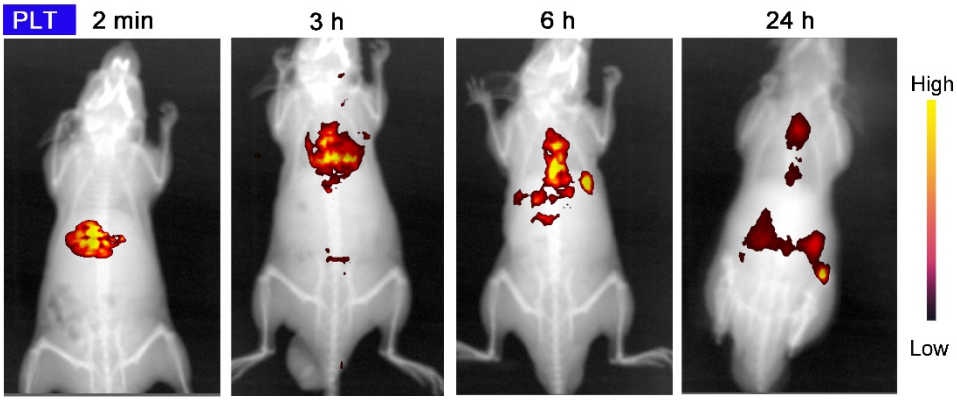

Fig. S7 *In vivo* imaging and bio-distribution of PLT carrier after the intravenous injection.

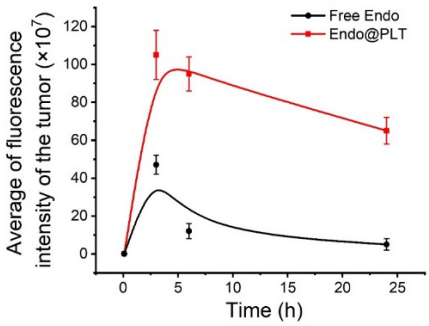

Fig. S8 The average fluorescence intensity of the tumors after intravenous injection, Cy5 labeled Endo was used for preparing Endo@PLT. The Cy5 Endo@PLT were separately injected into C57BL/6 mice bearing the LLC tumor, and fluorescence in tumor tissue was monitored at different time points. The fluorescence intensity of free Endo declined over the experimental time because of clearance. The Edno@PLT treated group showed accumulation in the lung (tumor) remained strongly fluorescent over time, indicating the Endo@PLT accumulation in the tumor.

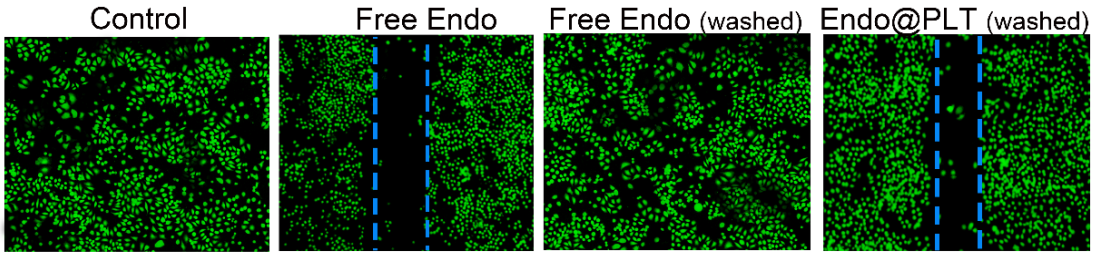

Fig. S9 Representative images of the wound healing assay for Endo and Endo@PLT treatments compared to the untreated group in LLC cells.

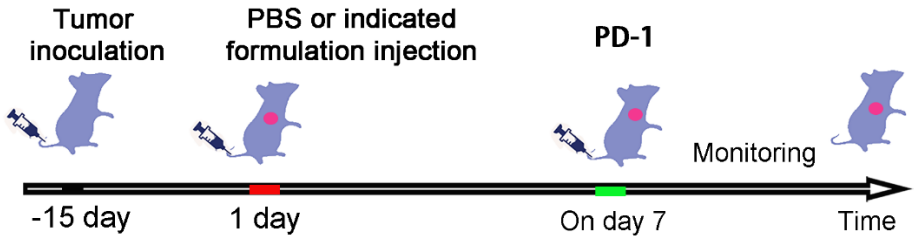

Fig. S10 The treatment schedule used for Endo@PLT-mediated combination therapy against a subcutaneous LLC tumor.

Staining for the endothelial cell marker CD31 showed that not only the average vessel area was reduced significantly after Endo@PLT treatment, the vessel morphology was also changed (Fig. 3A and Fig.S9). Tumor vessels from control group, Endo, PLT and Endo+PLT, followed serpentine course with irregular and heterogeneous structures. Meanwhile tumors were less hypoxic, as assessed by staining of VEGF whose accumulation and activity is precisely regulated by the cellular O_2 concentration (Fig. 3A and Fig.S9).

Thirty tumor-bearing mice were randomly divided into three groups and treated through tail-vein injection. (1) Group1, the Endo@PLT without separation. (2) Group 2, the unbound Endo isolated from Endo@PLT supernatants. (3) Group 3, the Endo@PLT after separation (Fig. S10A). After 7 days, mice in each group were sacrificed to investigate hypoxia. The lung sections were stained with hematoxylin and eosin and immune-stained for CD31 measurements.

The results are displayed in Fig. S10 B and C, the group 2 (unbound Endo isolated from Endo@PLT supernatants) caused less efficacy in vascular normalization after 7 days, may be due to the short half-life of Endo (about 10 h). By contrast, Endo@PLT with or without separation treatments groups showed less red fluorescence after CD31 staining. It is reasonable to believe that the improvement of vascular functionality is attributed to the Endo@PLT.

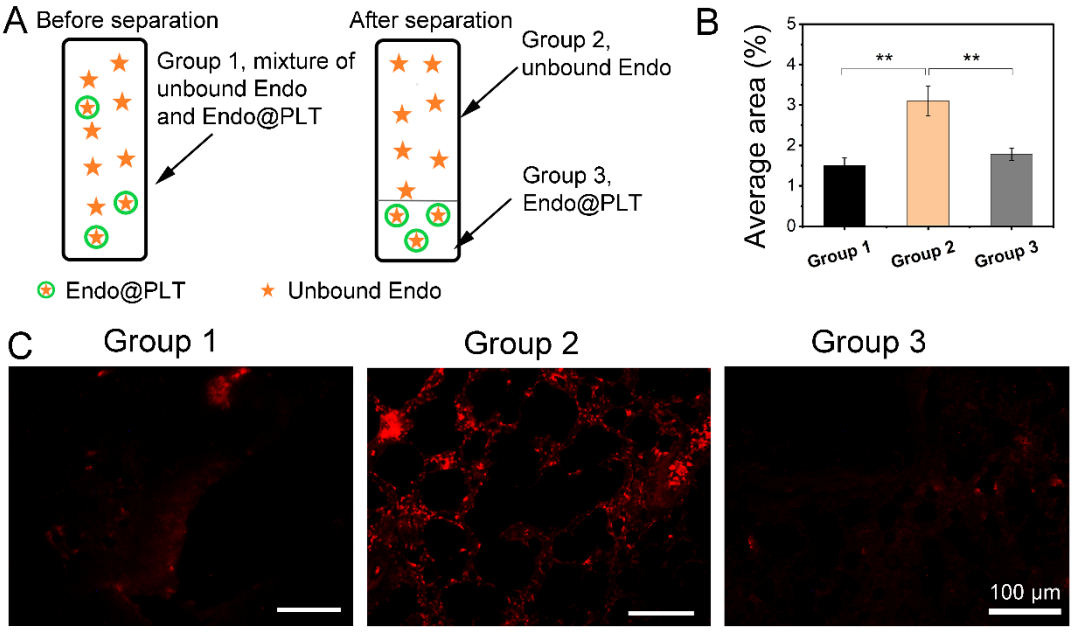

Fig. S11 The vascular normalization efficacy. (A) The grouping was as follows, (1) Group1, the Endo@PLT without separation. (2) Group 2, the unbound Endo isolated from Endo@PLT supernatants. (3) Group 3, the Endo@PLT after separation. (B) Representative immunofluorescence quantitative analysis after staining for CD31. (C) Representative immunofluorescence microscopic images of tumor sections after staining for CD31. Sale bar =100 μm. ** P<0.01

It can be found that CD31 and VEGF were not affected by Endo, PLT or Endo+PLT. Therefore, we speculated that the using PLT to entrap the Endo in the tumor therapy, can effectively mitigate the hypoxia in tumor tissue.

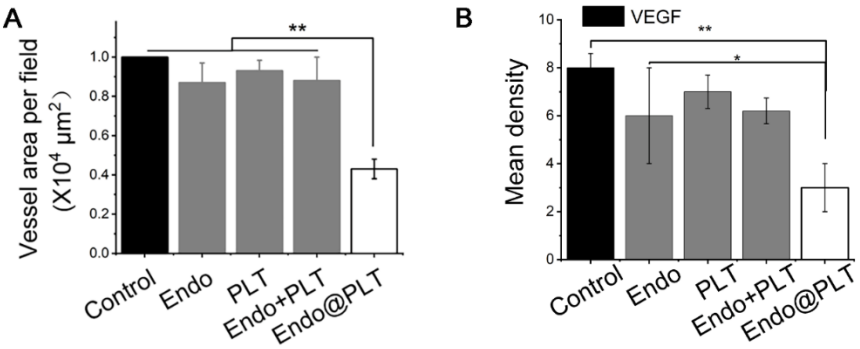

Fig. S12 Representative immunofluorescence quantitative analysis after staining for CD31 (A) and VEGF (B). After 7 days of treatment, tumor tissues were cryo-sectioned and immune-stained for CD31. The Endo@PLT treatment caused vascular normalization, coinciding with decreased hypoxia as revealed by the lower VEGF levels. ** $P < 0.01$, * $P < 0.05$.

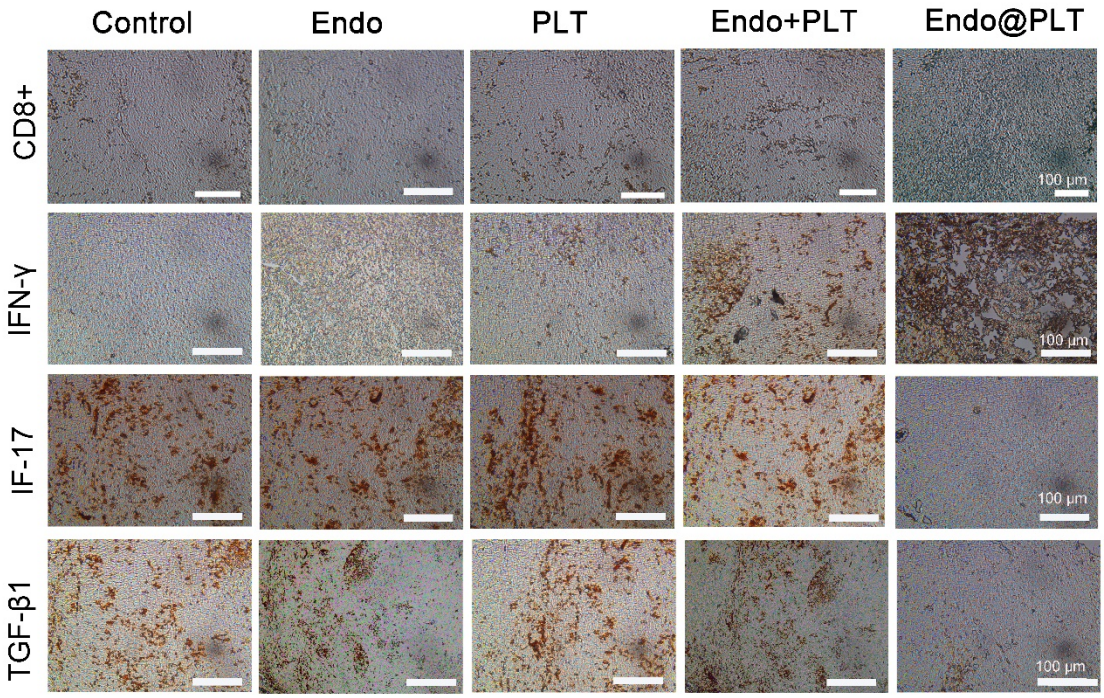

Fig. S13 Immunofluorescence images of $CD8^+$ protein, INF-γ, IF-17, and TNF-β1 areas in LLC tumors after treatment.

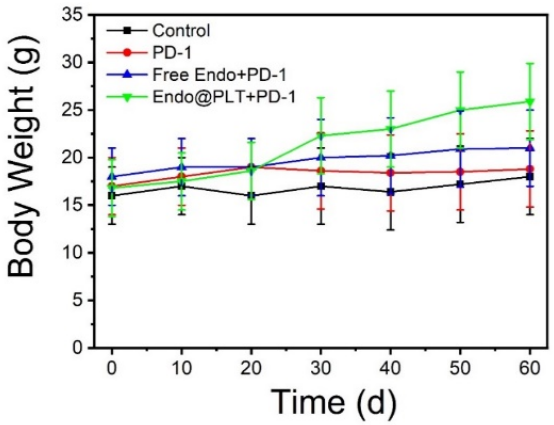

Fig. S14 The body weight curves of all test groups. No significant effect on body weight increase were observed during the study

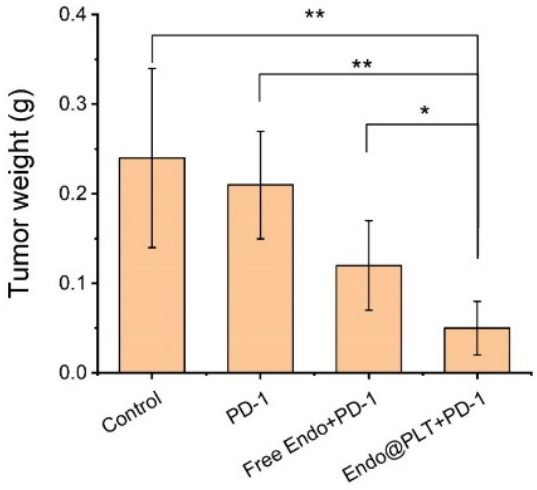

Fig. S15 The weight of recurrent tumors of all groups. The tumor weight in Endo@PLT + PD-1 group were markedly reduced as compared with the control group. * P<0.05; ** P<0.01.

The *in vivo* biological safety of the Endo@PLT+PD-1 was evaluated. On day 60 after treatment with Endo@PLT+PD-1, mice were killed, and histology analyses of the heart, liver, kidney, and spleen were performed by a typical hematoxylin and eosin (H&E) method. The H&E staining displayed nondetectable lesions such as hydropic degeneration, inflammatory, and pulmonary fibrosis in the tissue sections (Fig. S16, and S17), suggesting that Endo@PLT+PD-1 did not cause damage in these organs.

Routine blood examinations showed that total red blood cells (RBC) count, hemoglobin levels (HGB), platelets (PLT), and the total white blood cells (WBC) count maintained a normal range after PD-1, free Endo+PD-1, and Endo@PLT+PD-1 treatment (Fig. S18A). The liver function markers such as ALP, ALT, and AST and the kidney function markers such as BUN, GLB and Cr, were normal during the test procedure (Fig. S18B), suggesting no apparent hepatic and kidney disorders in mice after Endo@PLT+PD-1 treatment and confirming the excellent biocompatibility of Endo@PLT+PD-1 *in vivo*.

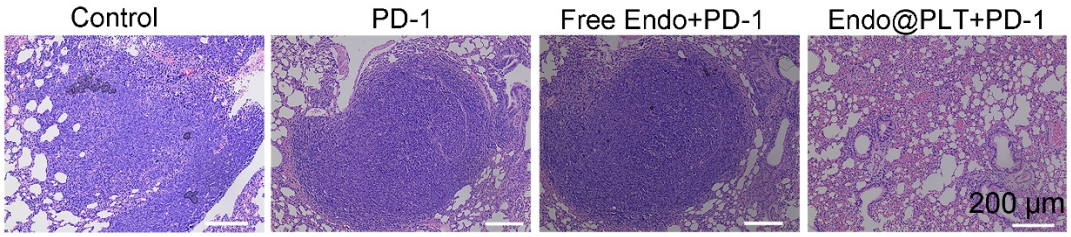

Fig. S16 H&E staining of lungs from indicated groups of mice at the end of the study. Each scale bar = 200 μm.

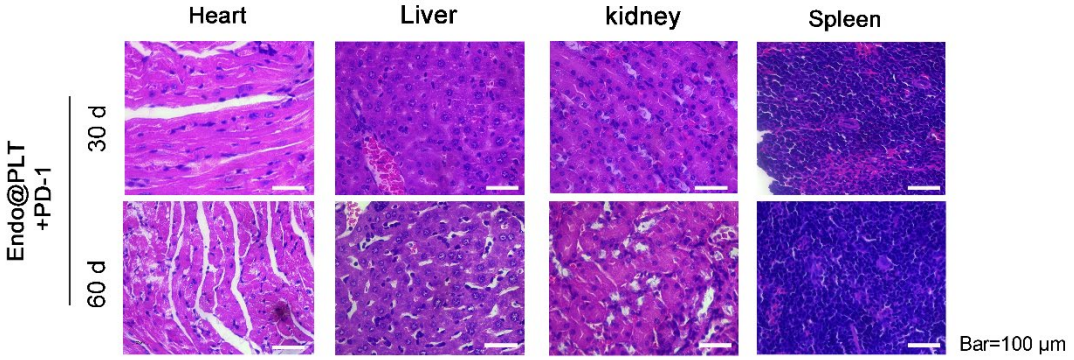

Fig. S17 Biosafety evaluation results. H&E staining of sections of the main organs, including the heart, liver, kidney, and spleen, after the Endo@PLT+PD-1 treatment.

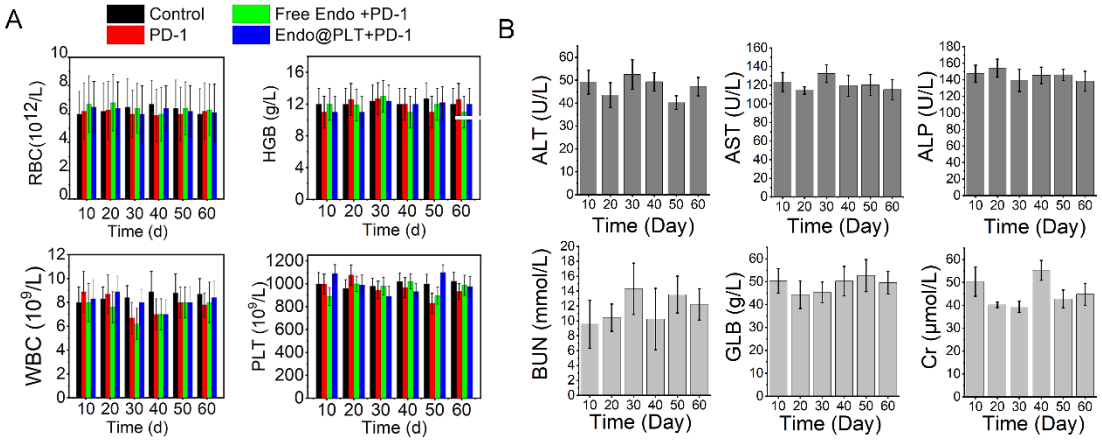

Fig. S18 Biosafety evaluation results. (A)Variations in the complete blood parameters, (B) parameters of serum biochemistry profiles for 10, 20, 30, 40, 50, and 60 days.

Reference

1. D. Xia, D. Hang, Y. Li, W. Jiang, J. Zhu, Y. Ding, H. Gu and Y. Hu, *ACS nano*, 2020, **14**, 15654-15668.

2. R. S. Qin, Z. H. Zhang, N. P. Zhu, F. Chen, Q. Guo, H. W. Hu, S. Z. Fu, S. S. Liu, Y. Chen, J. Fan and Y. W. Han, *BMC cancer*, 2018, **18**, 967.
3. R. Liu, D. Li, B. He, X. Xu, M. Sheng, Y. Lai, G. Wang and Z. Gu, *Journal of controlled release : official journal of the Controlled Release Society*, 2011, **152**, 49-56.
4. Y. J. Liang, H. Yu, G. Feng, L. Zhuang, W. Xi, M. Ma, J. Chen, N. Gu and Y. Zhang, *ACS applied materials & interfaces*, 2017, **9**, 43478-43489.
5. M. Chhatriwala, R. G. Ravi, R. I. Patel, J. L. Boyer, K. A. Jacobson and T. K. Harden, *The Journal of pharmacology and experimental therapeutics*, 2004, **311**, 1038-1043.